NC2 mobilizes TBP on core promoter TATA boxes

Peter Schluesche¹, Gertraud Stelzer², Elisa Piaia², Don C Lamb^{1,3} & Michael Meisterernst^{2,4}

The general transcription factors (GTFs) of eukaryotic RNA polymerase II, in a process facilitated by regulatory and accessory factors, target promoters through synergistic interactions with core elements. The specific binding of the TATA box-binding protein (TBP) to the TATA box has led to the assumption that GTFs recognize promoters directly, producing a preinitiation complex at a defined position. Using biochemical analysis as well as biophysical single-pair Förster resonance energy transfer, we now provide evidence that negative cofactor-2 (NC2) induces dynamic conformational changes in the TBP-DNA complex that allow it to escape and return to TATA-binding mode. This can lead to movement of TBP along the DNA away from TATA.

The general initiation factors and RNA polymerase II target core promoter regions after opening of the chromatin structure. A wellstudied early step in initiation of transcription is the specific binding of TBP to core-promoter TATA boxes, which is enhanced by the general initiation factor TFIIA¹. Assembly of the preinitiation complex on promoters that do not contain a TATA sequence more crucially depends on synergistic interactions of GTFs and associated factors (such as TAFs) with other core promoter elements (INR, BRE, DCE, DPE and MTE)^{2–7}. When the preinitiation complex forms, it remains in position at the core promoter until RNA polymerase II clears the promoter; at this point, general factors, with the possible exception of TBP, dissociate⁸. This widely accepted model of transcription complex assembly is static in the sense that initiation factors such as TBP must bind directly to the site where initiation complexes are formed, and if they erroneously bind an unproductive region, they must first dissociate before approaching the promoter from the nucleoplasm in a new attempt.

In this study, we have used yeast and human GTFs to investigate whether GTFs must indeed target core promoters directly at the sites of initiation or whether GTF-DNA interactions involve dynamic processes such that factors can move along the promoter DNA. Our results extend the static picture of complex assembly by demonstrating that TBP is mobilized on DNA upon binding of the transcription cofactor NC2 (also called Dr1-DRAP)^{9,10}.

NC2 is an evolutionary conserved protein complex^{11,12} that binds TBP–DNA from the bent underside on TATA. The cofactor forms a ring-like structure with TBP¹³, which sterically occludes association of TFIIA and TFIIB^{13–15}. The NC2 complex facilitates interactions of TBP with both TATA and non-TATA binding sites. It is present on a substantial fraction of all active human genes¹⁷ and is thus an excellent candidate for mediating the stable binding and final positioning of

TBP. Genetic studies have revealed both negative and positive effects of NC2 on gene expression^{18–21} (reviewed in ref. 22). The mechanism underlying the positive effects of NC2 *in vivo* is not understood.

Here we suggest that NC2 helps to maintain TBP on promoter regions. The cofactor markedly decreases the off-rate of TBP from DNA. To our surprise, we also observed that NC2 induces rapid dynamic changes in the conformation of the TBP–DNA complex. Moreover, a fraction of TBP escapes from the TATA region upon formation of a complex with NC2. Collectively, the data suggest that the factor not only binds and stabilizes TBP to retain the initiation factor in promoter regions, but also mobilizes TBP on the DNA. This offers a molecular framework for prediction of a variety of inhibitory and enhancing gene regulatory modes of NC2 that may broaden the regulatory repertoire of eukaryotic cells.

RESULTS

NC2 binding alters TBP-TATA interactions

The first indications that TBP-TATA interactions loosen upon encountering NC2 came from footprinting experiments. Addition of NC2 to a preformed TBP adenovirus major late (AdML) TATA promoter complex caused gradual loss of the protected window at TATA with increasing NC2 concentrations (Fig. 1a). Loss of TATA protection was rapid (complete in less than 1 min) and was seen on both strands of the DNA (Fig. 1b). The effect occurred with both recombinant and native NC2 complexes (Supplementary Fig. 1a online), with both human and yeast TBP, and in both the absence and presence of TFIIA and TFIIB (Supplementary Fig. 1b,c). The loss of TATA protection was also seen in copper-phenanthroline footprinting, indicating that this phenomenon is not specific to DNase I digestion (Supplementary Fig. 1d and ref. 23). The effect is, however, specific to the NC2 complex: it is not seen in the presence of even an excess of

Received 15 April; accepted 2 October; published online 11 November 2007; doi:10.1038/nsmb1328



¹Department of Chemistry and Biochemistry and Center for Nanoscience (CeNS), Ludwig Maximilian University, Butenandtstr. 11, 81377 Munich, Germany.
²Helmholtz Center Munich German Research Center for Environmental Health, Gene Expression Marchionini-Str. 25, 81377 Munich, Germany.
³Department of Physics, University of Illinois at Urbana-Champaign, 1110 West Green Street, Urbana, Illinois, 61801, USA.
⁴Institute for Cell and Tumor Biology, Department of Medicine, Westfalian Wilhelms University, 48149 Muenster, Germany. Correspondence should be addressed to M.M. (meisterernst@gsf.de) or D.C.L. (don.lamb@cup.uni-muenchen.de).

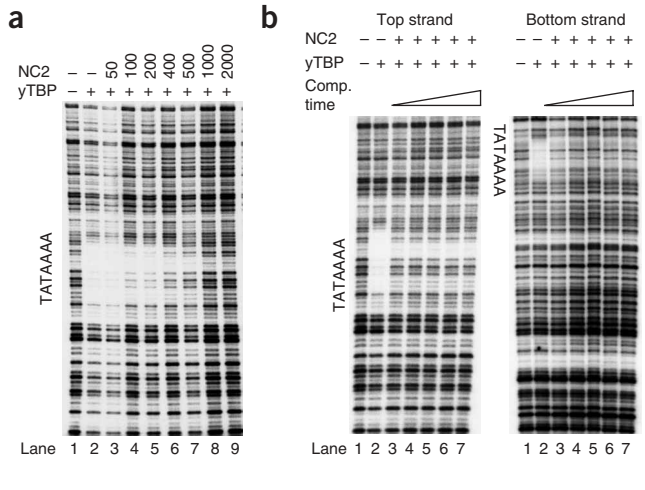


Figure 1 Loss of TBP–TATA protection against DNase I digestion mediated by NC2. (a) AdML 217-bp promoter fragment (100 fmol, 5 nM) was incubated with 350 fmol or 17.5 nM of yeast TBP (yTBP; for 30 min) and incubated with human NC2 (concentrations listed above gel in fmol per 20 μ l). (b) Time course (0.5, 3, 6, 15 and 40 min, lanes 3–7) of TATA clearance after the addition of NC2 (Comp.; 20 nM) to yTBP (17.5 nM) preincubated with DNA (5 nM) under standard conditions.

recombinant purified NC2 α or NC2 β subunits. Furthermore, it is not seen with the structurally related histone proteins H2A-H2B, which cover DNA nonspecifically (**Supplementary Fig. 1e**).

In the X-ray structure of the TBP-NC2-DNA complex, TATA is completely protected by TBP and NC2 (ref. 13). DNase I cannot cleave within the TATA motif unless the ring structure opens up (Supplementary Fig. 2a online). A trivial explanation for the observed access of DNase I to TATA would be the dissociation of TBP from the DNA upon encountering NC2. However, analysis of footprinting fractions using electrophoretic mobility shift assays (EMSAs) suggested that TBP remains fully bound to DNA in a complex with NC2 (Supplementary Fig. 2b-d). Furthermore, DNA competition measurements revealed a half-life in the range of one to several hours (Fig. 2 and Supplementary Fig. 3a,c online), approximately an order of magnitude longer than the half-life measured for TBP alone (Supplementary Fig. 3b). TBP was also retained on DNA when excess competitor DNA was added shortly before the addition of NC2 to a pre-formed TBP-TFIIA complex (data not shown). Hence, the loss of TATA protection cannot be explained by the dissociation of TBP molecules. Instead, the data suggest that the structure of the TBP-NC2-DNA complex must change. Two simple explanations can be envisioned: the ring-like protein structure formed by TBP and NC2 (Supplementary Fig. 2a) might open up, allowing DNase I access to TATA; alternatively, the TBP-DNA contacts might be weakened, allowing the conformation of the DNA to straighten and the TBP-NC2 complexes to move away from the TATA site.

Dynamic changes in TBP–DNA conformation upon NC2 binding To investigate the underlying molecular mechanisms, individual TBP–NC2–DNA complexes were studied by spFRET²⁴ using total internal reflection fluorescence microscopy (the experimental setup is shown schematically in **Supplementary Fig. 4** online). For spFRET experiments, we used recombinant mutant TBP from *Saccharomyces cerevisiae* that had a single cysteine at position 61 (ref. 25) labeled with a fluorescent donor molecule (Atto532), together with a 70-base-

pair (bp) AdML DNA labeled with an acceptor fluorophore (Atto647)

on the thymidine base 11 bp upstream of TATA (DNA-1 in **Supplementary Fig. 5a,b** online). We used concentrations of TBP and DNA that ensured only a single TBP molecule or TBP–NC2 complex was bound by each DNA.

Figure 3a shows the time dependence of a typical FRET signal from a TBP-TFIIA-DNA complex. More than 93% of the traces with a clear FRET signal showed a steady FRET value until photobleaching of either the donor or the acceptor molecule occurred. A histogram of FRET efficiencies for 631 TBP-TFIIA complexes (Fig. 3b) reveals two well-defined populations, one with a FRET efficiency of 0.40 and a smaller one (16% of all molecules) with a FRET efficiency of 0.21. The 0.40-FRET efficiency population corresponds to the TBP-DNA conformation observed in crystal structures. It is known that TBP can bind in two possible orientations²⁶. However, data collected either in the presence of TFIIA (which stabilizes the correct orientation) or with or without preincubation with TBP alone indicate that the alternative orientation of TBP corresponds to a population with a FRET efficiency of 0.56 (data not shown). Therefore, the 0.21-FRET population cannot represent another orientation on the same binding site as the 0.40-FRET population, but rather represents a second binding site.

Upon addition of NC2, the steady FRET signal from the TBP–DNA complex becomes dynamic, fluctuating rapidly between different FRET values (Fig. 3c). Of the complexes that had a clear FRET signal, 74% showed dynamic FRET upon the addition of NC2. This compares well with expectation that ~80% of TBP–DNA complexes interact with NC2 under these experimental conditions. TBP–NC2–DNA complexes continue to show dynamic FRET signals (for up to 4 h) after removal of excess NC2. Comparable results were obtained with a longer (110-mer) AdML-containing DNA labeled with a different acceptor molecule (Atto647N, Supplementary Fig. 5d–f). In both experiments, the transition from steady to dynamic FRET occurred without loss of the FRET signal, indicating that TBP does not dissociate from the DNA upon binding of NC2. The enhanced stability of TBP on the DNA upon binding with NC2 was also observed in single-molecule measurements (data not shown).

We performed extensive control experiments to investigate possible spurious causes of the dynamic signal observed. The transformation between steady FRET and dynamic FRET upon addition of NC2 was also evident when we used DNA labeled at different locations with different acceptor molecules (DNA-2 to DNA-4 in **Supplementary Fig. 5a–c**). Donor quenching did not influence the calculated FRET

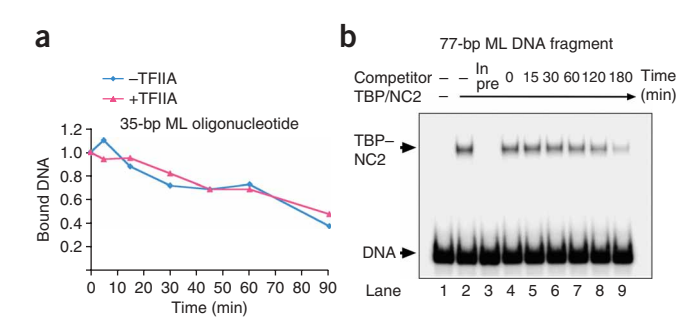
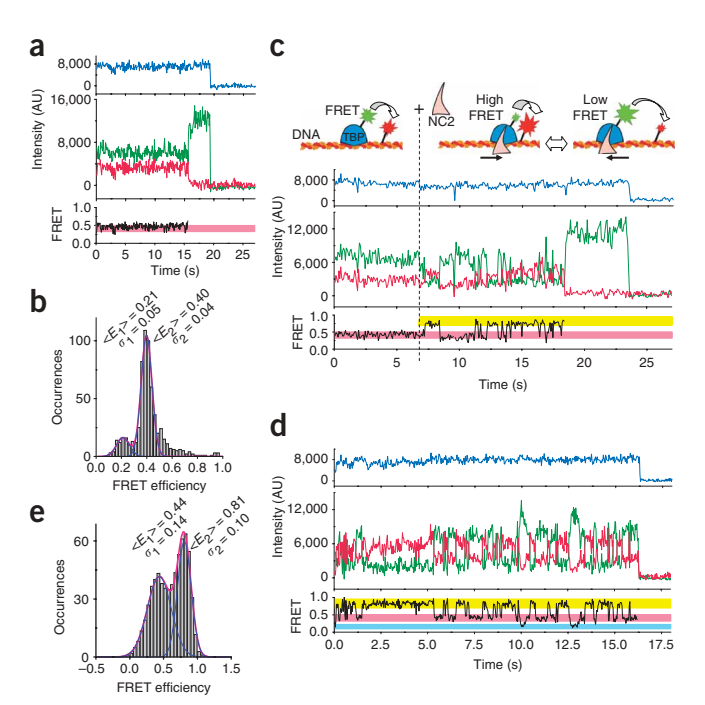


Figure 2 Half-life of TBP–NC2 on DNA. (a) Quantitative results of EMSAs showing competition of a 35-bp ML oligonucleotide preincubated with TBP–NC2 complexes in the presence or absence of TFIIA with a 500-fold molar excess of competitor DNA. (b) Half-life determination using a 77-bp ML fragment. The 77-bp ML DNA (3 nM) was incubated with yeast TBP (0.5 nM) and NC2 (1 nM) for 30 min at 28 °C and subjected to competition with a 37-bp ML oligonucleotide (3 μ M) for the indicated time periods. 'In pre', competitor DNA present in preincubation.





efficiency (**Supplementary Fig. 6a** online). The fluorescence intensity of the acceptor was monitored using millisecond alternating laser excitation (msALEX)²⁷ to verify that the photophysics of the fluorophores did not give rise to the observed dynamical behavior (**Supplementary Fig. 6b,c**). Anisotropy experiments confirmed that the orientations of the donor and acceptor dipoles were not responsible for the measured dynamics (**Supplementary Table 1** online). Further details are explained in the **Supplementary Discussion** online.

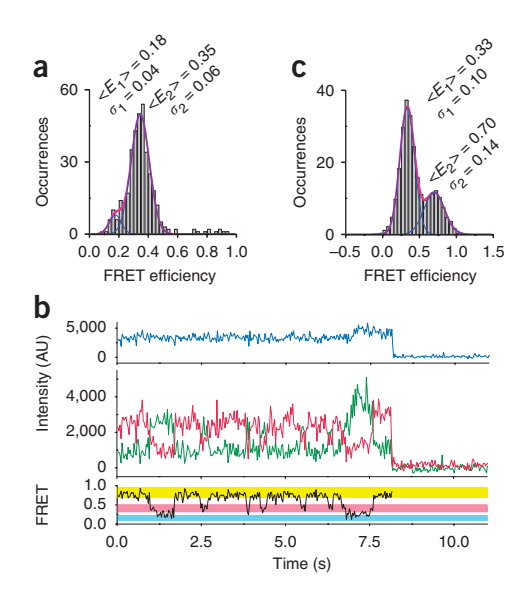
In a representative trace of TBP-NC2 dynamics at 30 ms per frame (Fig. 3d), the signal fluctuates between three FRET-efficiency regions (centered at 0.20, 0.40 and 0.80), suggesting the presence of at least three preferred binding sites and/or conformations of TBP-NC2 on the DNA. The histogram of FRET efficiencies per frame for 644 complexes (Fig. 3e) reveals an ~ 0.4 FRET population that is evident both before and after addition of NC2, suggesting that the conformation is similar in both cases. The expected distance between donor and acceptor attachment points for a bent TBP-TFIIA complex was estimated from the X-ray structure¹³ to be ~ 60 Å, which agrees well with the 64 Å calculated from our 0.4-FRET efficiency peak. The 0.8 peak involves a change in conformation of the DNA. DNA straightened out into a B-form structure would correspond to a FRET efficiency somewhere between 0.60 and 0.88. As the 0.8 peak observed is in this range, any movement of the TBP-NC2 complex along the DNA cannot be distinguished, by our methods, from the conformational changes of the DNA. Experiments were also performed with both the donor and acceptor molecules attached to the DNA, but as the conformation of the DNA changes independently of movement of the TBP-NC2 complex, no additional information

Figure 4 Investigation of TBP–NC2 dynamics on DNA containing an H2B-J promoter. (a) Histogram of average FRET efficiencies for stable TBP–DNA complexes. E, mean value of gaussian fit; σ, s.d. of gaussian fit. (b) spFRET trace showing shuttling of the TBP–NC2 complex between different conformations on DNA containing the H2B-J promoter. Highlighted regions correspond to those in **Figure 3**. AU, arbitrary units. (c) Histogram of FRET efficiencies per frame from 259 TBP–NC2 complexes on H2B-J promoter DNA.

Figure 3 The fluorescence intensity and FRET-efficiency traces of single TBP-DNA complexes, before, during and after NC2 addition. (a) A typical measurement at 75 ms per frame before NC2 addition. Blue, total intensity $(\alpha I_{donor} + I_{acceptor}, where \alpha is the detection correction factor; see$ Supplementary Discussion); green and red, donor and acceptor intensities, respectively; black, FRET efficiency. The acceptor photobleaches first after ~ 15 s, and the donor photobleaches at ~ 20 s. AU, arbitrary units. (b) Histogram of average FRET efficiencies for stable TBP-DNA complexes. E, mean value of gaussian fit; σ , s.d. of gaussian fit. (c) Scheme of the experiment, and a 75-ms-per-frame spFRET trace taken during NC2 addition, showing a transition from steady to dynamic FRET behavior. (d) An spFRET trace taken at 30 ms per frame showing shuttling of the TBP-NC2 complex between three conformations and/or positions on the DNA. Cyan, 0.100-0.225 FRET efficiency; magenta, 0.325-0.500; yellow, 0.700-0.950. (e) A histogram of FRET efficiencies per frame from 644 TBP-NC2 complexes on AdML promoter DNA.

could be gained from these measurements. However, the state around 0.2 FRET efficiency cannot be explained by modeling of the DNA conformation and may indicate movement of the TBP–NC2 complex to a position further downstream on the AdML promoter. It is currently unclear whether this state relates to the minor population of 0.21 FRET efficiency seen with TBP–TFIIA alone (Fig. 3b).

To verify that the observed dynamics is not specific to the AdML promoter, we also measured spFRET on DNA containing the H2B-J promoter (sequence shown in Supplementary Fig. 7a online). As before, the TBP-DNA complexes showed steady-state FRET behavior with the main peak at a FRET efficiency of 0.35 (Fig. 4a). The absolute FRET values diverged from those measured with the AdML promoter because of the different labeling position of the acceptor and potentially any other changes caused by the different TATA sequence at the H2B-J promoter. The FRET behavior switched to a dynamic FRET signal upon addition of NC2 (Fig. 4b). Again, multiple FRET states were evident in the dynamic FRET signal. The per-frame histogram of FRET efficiencies for 259 complexes is shown in Figure 4c. The histogram shows a major state with a FRET efficiency around 0.33, again suggesting that TBP-NC2-DNA adopts a similar conformation to that of the TBP-TFIIA-DNA complex. The minor state on H2B-J with a FRET efficiency of 0.70 is less well represented than the corresponding population of AdML with a FRET efficiency of 0.81 (Fig. 3e), suggesting subtle promoter-specific differences in the







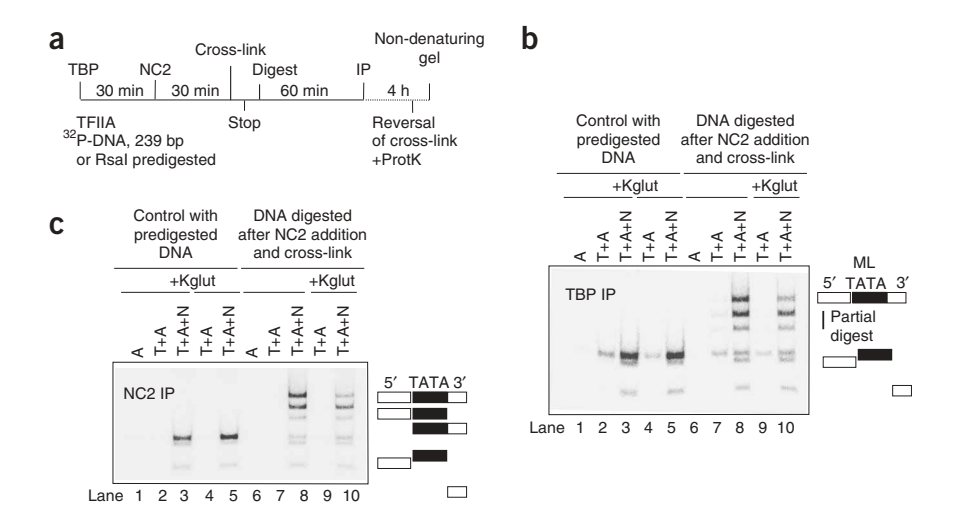


Figure 5 CRIP analysis of TBP-TFIIA and TBP-NC2 complexes. (a) Scheme for the CRIP experiments. (b) TBP-specific immunoprecipitation (IP) of reactions (in the presence or absence of physiological salt (potassium glutamate, Kglut) concentrations) containing human TBP (T, 23 nM), TFIIA (A, 16 nM), a 239-bp AdML fragment (predigested with RsaI, lanes 1-5; or digested after incubation with NC2 and cross-linking, lanes 6-10) and NC2 (N, 150 nM). Positions of central (99 bp, TATA), and flanking (88 and 52 bp) fragments are indicated. (c) CRIP experiment as in b but with NC2-specific immunoprecipitation.

dynamic behavior. The change in the relative populations observed in the dynamic FRET traces suggests subtle promoter-specific differences in the dynamic behavior.

Movement of TBP-NC2 complexes along DNA

To further investigate whether TBP-NC2 complexes can move along DNA, we developed a cross-linking restriction digest-coupled immunoprecipitation (CRIP) assay. The rationale of this CRIP assay (schematically summarized in Fig. 5a) is to determine roughly the position of a mobile complex on a longer DNA fragment. TBP and TFIIA were preincubated with a randomly radioactively labeled 239-bp AdML DNA fragment. After incubation with NC2, complexes were crosslinked with formaldehyde. The template was then digested with suitable enzymes, and protein-DNA complexes were immunoprecipitated and purified. The proteins were removed from the DNA with proteinase K and the resulting labeled DNA fragments were analyzed on nondenaturing PAA gels, on which they could be discriminated by size.

Figure 5b,c shows parallel CRIP experiments for immunoprecipitations with TBP and NC2 antibodies, respectively. In both the TBP immunoprecipitation assay (Fig. 5b, lanes 2-5 and 7-10) and the NC2 immunoprecipitation assay (Fig. 5c, lane 3, 5, 8 and 10), positive signals were restricted entirely to the lanes that contained the respective antigens. As controls for nonspecific stabilization of TBP by NC2, RsaIpredigested ML promoter DNA was processed in parallel (Fig. 5b,c, lanes 1-5), and reactions were also conducted at physiological salt

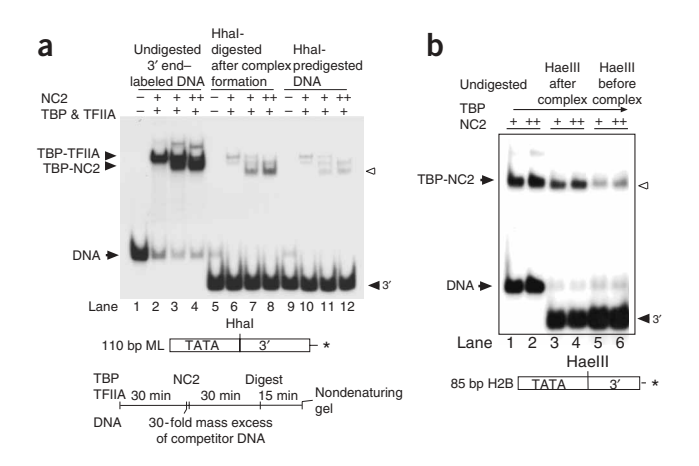
Figure 6 RCE analysis of TBP-NC2 complexes. (a) TBP (4.25 nM) was preincubated with TFIIA (6 nM) and a 110-bp AdML fragment (5 nM) labeled (asterisk represents radiolabel) at the 3' end, and then NC2 was added (2 nM in lanes 3, 7 and 11; 10 nM in lanes 4, 8 and 12). Undigested DNA (lanes 1-4), DNA digested with Hhal after complex formation (lanes 5-8, 20 units Hhal) and Hhal-predigested DNA (lanes 9-12, see scheme below) were used. Carrier DNA (37-bp ML oligonucleotide, $0.05 \mu M$) was added 1 min before addition of NC2. Open arrowhead indicates the position of TBP-NC2 bound to the labeled 3' Hhal fragment. (b) RCE analysis of TBP-NC2 on the H2B-J core promoter region. TBP was prebound to a synthetic 85-mer oligonucleotide or HaelII-predigested DNA.

concentrations (Kglut). Before the addition of NC2, TBP is present on the TATA fragment (Fig. 5b, lanes 7 and 9). Upon addition of NC2, TBP-NC2 complexes appear in the DNA fragments located upstream and downstream of TATA (Fig. 5b, lanes 8 and 10). Virtually identical patterns were seen for TBP-NC2 complexes in the TBP immunoprecipitation and NC2 immunoprecipitation experiments (compare lanes 3 and 8 in Fig. 5b,c), supporting the idea that it is the TBP-NC2 complex that we are detecting. Notably, redistribution of TBP-NC2, indicated by the relative decrease in TATAfragment occupancy, was seen only when undigested templates were used in the reactions (Fig. 5b,c, compare lanes 3 and 5 with lanes 8 and 10). The redistribution of TBP was efficient at NC2 concentrations closer to physiological conditions (100-200 nM; Supplementary Fig. 8 online), a result that corresponded well with our footprinting analysis (Fig. 1a). Redistribution was not prevented when a 300-fold molar excess of competitor DNA was introduced a few seconds before the

addition of NC2, which indicates that TBP can relocalize without dissociating from the DNA template (Supplementary Fig. 8).

Movement confirmed by restriction digest-coupled EMSA

To further confirm that complexes move along the DNA, we used a restriction digest-coupled EMSA (RCE) assay. We formed TBP-TFIIA complexes on DNA, then added carrier DNA and NC2. The sample was then subjected to a short restriction digest and the products were directly analyzed in EMSAs. To keep the situation simple, we used a 3' end-labeled version of the 110-bp synthetic AdML DNA from the experiments described above (see scheme in Fig. 6a). Undigested DNA (Fig. 6a, lanes 1-4) was compared with HhaI-predigested DNA (Fig. 6a, lanes 9-12) and DNA digested with HhaI after addition of NC2 (Fig. 6a, lanes 5-8). A residual 3% of the total NC2 (relative to the amount bound to the intact fragment in Fig. 6a, lane 4, lowest band) was found on predigested DNA (Fig. 6a, lane 12), whereas about 11% of the total NC2 localized to 3' ends if templates were digested after incubation of TBP-TFIIA with NC2 (Fig. 6a, lane 8). Thus, after subtraction of the background (Fig. 6a, lane 12), approximately 8% of the complexes were found to fully redistribute to the end of the DNA.



We also investigated movement of the TBP–NC2 complex away from the TATA box in spFRET experiments using DNA carrying acceptor labels attached to both ends (**Supplementary Fig. 5a.g.h**). In good accordance with the EMSA results, a statistical analysis of 1,682 complexes showed a 16% increase in complexes that had a detectable FRET signal between the ends of the DNA after addition of NC2.

Therefore, we conclude that a fraction of the TBP–NC2 complexes move along the DNA to flanking regions. This is not restricted to the major late promoter, as it was also seen on the cellular H2B-J promoter, which has previously been shown to harbor substantial amounts of NC2 throughout the cell cycle¹⁷. If templates were digested after TBP–NC2 complex formation, increased amounts of TBP–NC2 complex were seen downstream of the H2B TATA box upon addition of NC2 (**Fig. 6b**). DNase I footprinting results revealed changes in the protection of the TATA region (**Supplementary Fig. 7b**), although the region near TATA was not fully accessible to DNase I under the conditions we used. This indicates that TBP bound to other promoters is affected in a similar way upon NC2 binding; however, there could be subtle differences that may, for example, relate to the context in which TATA is embedded and the positions of preferred TBP–NC2–binding sites within the promoter regions (G.S. and M.M., unpublished data).

DISCUSSION

Previous spFRET studies of the transcription machinery have investigated static complexes^{28–30}. Our investigation represents the first spFRET analysis of the dynamics of a sequence-specific GTF. Our data suggest that the TBP–DNA complex undergoes dynamic changes upon encountering NC2 that occur in discrete steps. At least a fraction of complexes can leave TATA and relocalize to flanking regions. Physical prerequisites for transport from TATA to flanking binding sites are the ring-like structure seen in the X-ray analysis (**Supplementary Fig. 5a**) and the high affinity of TBP–NC2 for nonspecific DNA¹⁶. Contrary to previous reports³¹, TBP moves along DNA only after forming a complex with NC2.

The long half-life of TBP–NC2 complexes is not consistent with free diffusion of the complexes along the DNA. Instead, TATA and perhaps other sequences (compare **Supplementary Fig. 1e** to **Supplementary Fig. 7b**) remain preferred recognition sites. Consistent with this hypothesis, mutations of TATA in short oligonucleotides abolished binding of TBP–NC2 in solution (C. Goebel and M.M., unpublished data), whereas such mutations had no detectable effect in the context of a 240-bp DNA fragment¹⁶. This is also suggested by the X-ray structure, which shows TBP–NC2 in a complex with a TATA oligonucleotide. We propose that the short 19-mer oligonucleotide prevents both conversion into a non-bent mode and lateral movements.

At the present stage of our investigations, we can only speculate about the mechanism(s) leading to complex opening and movement along DNA. Our favored model involves changes in the DNA conformation during this process. The two major populations observed in FRET may be explained by a bent and a non-bent DNA conformation in the complex. An increase in DNA flexibility would also explain why TBP–NC2–DNA is more mobile than TBP–TFIIA–DNA in non-denaturing gels. The latter factors force TATA into a roughly 80° bending angle in solution (**Fig. 5d,g** and G.S. and M.M., unpublished data), which is consistent with the X-ray structure. Changes in the DNA conformation of TBP–NC2–DNA complexes are also likely from an energetic point of view, because the minor groove is highly distorted in the complex.

Our data has revealed a novel molecular function of NC2. We hypothesize that changing the conformation of TBP-DNA complexes inhibits the association of TFIIB and, therefore, leads to enhanced

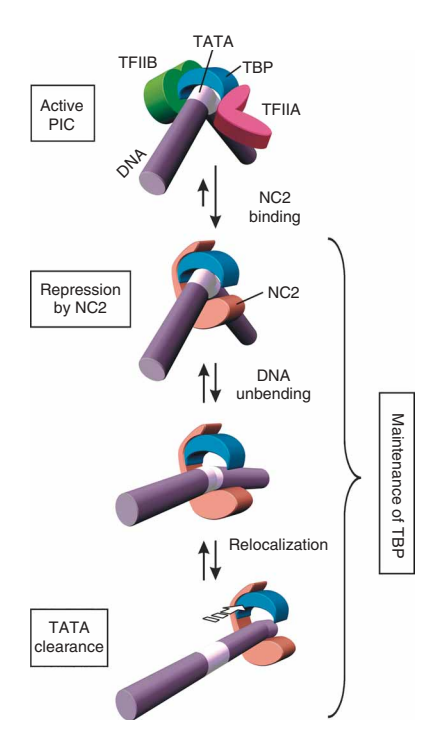


Figure 7 Model for TBP–NC2 complex dynamics and its consequences for preinitiation complex formation at TATA or altered preferred promoter recognition sites. NC2 competes with transcription factors such as TFIIA and TFIIB for binding to TBP, leading to repression of gene expression and in parallel with maintenance of TBP at promoters. Upon binding of NC2, the TBP–DNA complex opens, allowing the TBP–NC2 complex to relocate on the DNA. Movement of the TBP–NC2 complex could theoretically enhance gene expression by clearing TATA for other factors or by relocating the TBP to another promoter site where transcription can occur. Alternatively, or in addition, NC2 may also be involved in preinitiation complex recycling and/or licensing of transcription.

repression by NC2. Relocalization of the complex could result in even more efficient repression. Alternatively, or in addition, the NC2-mediated dynamic conformational changes in TBP–TATA and TBP clearance of TATA may pave the way for alternative constructive mechanisms in gene control (**Fig. 7**). For example, we hypothesize that the capacity to dynamically rearrange the structure and move TBP over short distances could help in assembling the complex at the optimal position for initiation (**Fig. 7**). This is conceptually distinct from the widely accepted assumption of direct assembly and disassembly of GTFs at core promoters of class II genes. Last but not least, the extremely low off-rate of TBP–NC2 is noteworthy. It will be of interest to evaluate the effects of the stability of this complex in keeping promoters accessible and occupied with TBP for long time periods.

METHODS

Proteins. Purified recombinant yeast and human TBP, yeast TFIIA (Toa1 and Toa2) and His-tagged NC2 subunits were expressed and purified as described 16. Active concentrations, as determined in gel-shift experiments, are given in the figure legends.

DNase footprinting and electrophoretic mobility shift assays. Standard procedures were applied as described^{14,19}, with variations detailed in **Supplementary Methods** online.

Cross-linking restriction digest–coupled immunoprecipitation assay. DNA fragments were internally labeled using ³²P-dCTP in PCR reactions, purified



and incubated with purified recombinant proteins under standard *in vitro* transcription conditions for 30–60 min at 28 °C. Details are given in **Supplementary Methods**. In brief, reactions were cross-linked using 1% (w/v) CH₂O and stopped with 1 volume of 300 mM glycine (pH 7.0). The volume was expanded and samples were digested with restriction enzyme for 1 h at 37 °C. Blocked protein G beads were loaded with antibodies, washed and incubated with the samples for 4–14 h at 6 °C in immunoprecipitation buffer. Beads were washed several times with excess TBST (10 mM Tris (pH 8.0), 150 mM NaCl, 0.05% (v/v) Tween 20) at 0 °C, incubated in elution buffer for 10 min at 65 °C and subjected to cross-link reversal at 65 °C overnight, and proteins were digested with proteinase K for 2 h at 56 °C. The samples were loaded on nondenaturing 6% (w/v) PAA gels without further purification and subjected to standard electrophoresis conditions.

Restriction digest—coupled electrophoretic mobility shift assay. TBP (2–5 nM) was incubated with synthetic (ML or H2B) promoter DNA fragments (5–10 nM), radioactively labeled on one end and carrying a single restriction site between TATA and the labeled end of the DNA. A 30-fold molar excess of carrier oligonucleotide containing ML TATA was added, followed by NC2 (2–10 nM); the mixture was incubated for 30 min at 28 °C and then combined with 2 volumes restriction buffer and digested with the enzymes indicated in the figure legends for 15 min at 37 °C. Samples were loaded on native 6% (w/v) 37.5:1 acrylamide/bisacrylamide TBE gels, and the amount of TBP-NC2 bound to the labeled DNA fragment lacking TATA was measured. Experiments performed with predigested DNA served as a control for complex formation independent of movement along the DNA.

Single-pair Förster resonance energy transfer. The single-cysteine mutant of yeast TBP was specifically labeled with maleimide-functionalized Atto532 (Atto-Tec) as FRET donor. The DNA strands were ordered from IBA BioTAGnology and were already labeled with the FRET acceptor Atto647, Atto647N or Alexa647 at various positions and with a biotin tag at one end of the DNA strand (exact positions are given in Supplementary Figs. 5 and 7). A mixture of 10 nM DNA, 5-10 nM TBP and 20 mM TFIIA was allowed to preincubate for 15 min at 28 °C in working buffer (for details, see **Supplementary Methods**). Before addition of the sample to the flow chamber (probe volume \sim 6 μ l), the sample was diluted to a concentration of 30 pM of complex. To prevent nonspecific adsorption of the probe to the quartz surface, the sample chamber was silanized and covered with poly(ethylene glycol). The TBP-DNA-TFIIA complexes were bound to the surface by a PEG-biotin-streptavidin-biotin-DNA linkage. Excess complex was removed after 5 min by rinsing with working buffer. SpFRET experiments were performed with a home-built prism-type total internal reflection fluorescence microscope (modified TE2000-U, Nikon) with dual-color detection by an EM-CCD camera (iXon DV 887-ECS, Andor Technology). The experimental setup is shown schematically in Supplementary Figure 4. The sample was excited with a Nd:YAG laser (532 nm, CrystaLaser) and a HeNe laser (633 nm, Laser 2000) was used in addition for the msALEX experiments²⁷. Data were typically recorded with a temporal resolution of 30 or 75 ms per frame. A home-built microflow system was used to automatically control the addition of NC2 during measurements. Excess NC2 was removed after 5 min by rinsing with working buffer. More detailed information regarding protein labeling, surface modification, flow-chamber preparation, microscope setup, data analysis and control experiments can be found in Supplementary Methods.

Note: Supplementary information is available on the Nature Structural & Molecular Biology website.

ACKNOWLEDGMENTS

We thank C. Goebel for excellent technical assistance, A. Lammens and D. Niessing for help with modeling of the TBP–DNA structure, T. Weil (Vanderbilt University) for providing the single-cysteine mutant of TBP, R.G. Roeder, L. Tora, P. Cramer and C. Bräuchle for crucial advice, and J. Michaelis (Ludwig Maximilian University Munich) for providing the MatLab software. This work was supported by grants from the Ludwig Maximilian University, Center for Nanoscience (CeNS), the German Excellence Initiative via the Nanosystems Initiative Munich and the Center for Integrated Protein Science (CiPS) Munich, Helmholtz Center Munich German Research Center for Environmental Health, and the Deutsche Forschungsgemeinschaft (SFB 646) to M.M. and D.C.L.

AUTHOR CONTRIBUTIONS

P.S. built the single-molecule total internal reflection fluorescence microscope, performed all the single-molecule measurements, developed the analysis software and analyzed the single-molecule data. G.S. and E.P. performed biochemical analyses. D.C.L. and M.M. designed experiments and supervised the project.

Published online at http://www.nature.com/nsmb

Reprints and permissions information is available online at http://npg.nature.com/reprintsandpermissions

- Stargell, L.A., Moqtaderi, Z., Dorris, D.R., Ogg, R.C. & Struhl, K. TFIIA has activator-dependent and core promoter functions in vivo. *J. Biol. Chem.* 275, 12374–12380 (2000).
- Buratowski, S., Hahn, S., Guarente, L. & Sharp, P.A. Five intermediate complexes in transcription initiation by RNA polymerase II. Cell 56, 549–561 (1989).
- Thomas, M.C. & Chiang, C.M. The general transcription machinery and general cofactors. Crit. Rev. Biochem. Mol. Biol. 41, 105–178 (2006).
- Roeder, R.G. The role of general initiation factors in transcription by RNA polymerase II. Trends Biochem. Sci. 21, 327–335 (1996).
- Albright, S.R. & Tjian, R. TAFs revisited: more data reveal new twists and confirm old ideas. Gene 242, 1–13 (2000).
- Lewis, B.A., Sims, R.J., III, Lane, W.S. & Reinberg, D. Functional characterization of core promoter elements: DPE-specific transcription requires the protein kinase CK2 and the PC4 coactivator. *Mol. Cell* 18, 471–481 (2005).
- Wright, K.J., Marr, M.T., II & Tjian, R. TAF4 nucleates a core subcomplex of TFIID and mediates activated transcription from a TATA-less promoter. *Proc. Natl. Acad. Sci. USA* 103, 12347–12352 (2006).
- Sims, R.J., III, Mandal, S.S. & Reinberg, D. Recent highlights of RNA-polymerase-Il-mediated transcription. *Curr. Opin. Cell Biol.* 16, 263–271 (2004).
- Meisterernst, M. & Roeder, R.G. Family of proteins that interact with TFIID and regulate promoter activity. Cell 67, 557–567 (1991).
- Inostroza, J.A., Mermelstein, F.H., Ha, I., Lane, W.S. & Reinberg, D. Dr1, a TATA-binding protein-associated phosphoprotein and inhibitor of class II gene transcription. Cell 70, 477–489 (1992).
- Iratni, R. et al. Inhibition of excess nodal signaling during mouse gastrulation by the transcriptional corepressor DRAP1. Science 298, 1996–1999 (2002).
- Prelich, G. & Winston, F. Mutations that suppress the deletion of an upstream activating sequence in yeast: involvement of a protein kinase and histone H3 in repressing transcription in vivo. *Genetics* 135, 665–676 (1993).
- Kamada, K. et al. Crystal structure of negative cofactor 2 recognizing the TBP-DNA transcription complex. Cell 106, 71–81 (2001).
- 14. Goppelt, A., Stelzer, G., Lottspeich, F. & Meisterernst, M. A mechanism for repression of class II gene transcription through specific binding of NC2 to TBP-promoter complexes via heterodimeric histone fold domains. EMBO J. 15, 3105–3116 (1996).
- Mermelstein, F. et al. Requirement of a corepressor for Dr1-mediated repression of transcription. Genes Dev. 10, 1033–1048 (1996).
- Gilfillan, S., Stelzer, G., Piaia, E., Hofmann, M.G. & Meisterernst, M. Efficient binding of NC2.TATA-binding protein to DNA in the absence of TATA. J. Biol. Chem. 280, 6222–6230 (2005).
- Albert, T.K. et al. Global distribution of negative cofactor 2 subunit-alpha on human promoters. Proc. Natl. Acad. Sci. USA 104, 10000–10005 (2007).
- Gadbois, E.L., Chao, D.M., Reese, J.C., Green, M.R. & Young, R.A. Functional antagonism between RNA polymerase II holoenzyme and global negative regulator NC2 in vivo. *Proc. Natl. Acad. Sci. USA* 94, 3145–3150 (1997).
- Xie, J., Collart, M., Lemaire, M., Stelzer, G. & Meisterernst, M. A single point mutation in TFIIA suppresses NC2 requirement in vivo. EMBO J. 19, 672–682 (2000).
- Chitikila, C., Huisinga, K.L., Irvin, J.D., Basehoar, A.D. & Pugh, B.F. Interplay of TBP inhibitors in global transcriptional control. Mol. Cell 10, 871–882 (2002).
- Geisberg, J.V., Holstege, F.C., Young, R.A. & Struhl, K. Yeast NC2 associates with the RNA polymerase II preinitiation complex and selectively affects transcription in vivo. *Mol. Cell. Biol.* 21, 2736–2742 (2001).
- Klejman, M.P. et al. NC2alpha interacts with BTAF1 and stimulates its ATP-dependent association with TATA-binding protein. Mol. Cell. Biol. 24, 10072–10082 (2004).
- Auty, R. et al. Purification of active TFIID from Saccharomyces cerevisiae. Extensive promoter contacts and co-activator function. J. Biol. Chem. 279, 49973

 –49981 (2004).
- Myong, S., Rasnik, I., Joo, C., Lohman, T.M. & Ha, T. Repetitive shuttling of a motor protein on DNA. *Nature* 437, 1321–1325 (2005).
- Amitani, I., Baskin, R.J. & Kowalczykowski, S.C. Visualization of Rad54, a chromatin remodeling protein, translocating on single DNA molecules. *Mol. Cell* 23, 143–148 (2006)
- Cox, J.M. et al. Bidirectional binding of the TATA box binding protein to the TATA box. Proc. Natl. Acad. Sci. USA 94, 13475–13480 (1997).
- Kapanidis, A.N. et al. Alternating-laser excitation of single molecules. Acc. Chem. Res. 38, 523–533 (2005).
- Kapanidis, A.N. et al. Retention of transcription initiation factor sigma 70 in transcription elongation: single-molecule analysis. Mol. Cell 20, 347–356 (2005).
- Coban, O., Lamb, D.C., Zaychikov, E., Heumann, H. & Nienhaus, G.U. Conformational heterogeneity in RNA polymerase observed by single-pair FRET microscopy. *Biophys.* J. 90, 4605–4617 (2006).
- Kapanidis, A.N. et al. Initial transcription by RNA polymerase proceeds through a DNAscrunching mechanism. Science 314, 1144–1147 (2006).
- Coleman, R.A. & Pugh, B.F. Evidence for functional binding and stable sliding of the TATA binding protein on nonspecific DNA. J. Biol. Chem. 270, 13850–13859 (1995).